IJMT. Vol. 21, Iss. 1, 2025. (54-70)

International Journal of Maritime Technology

Journal homepage: ijmt.ir

Comparing the Effect of Duct Inlet Length on the Hydrodynamic Performance and Open Water Efficiency of a Pre-Swirl PumpJet Propulsion System with Experimental Method and Uncertainty Analysis

Mohammad Hossein Qaedsharaf [1], Ehsan Yari[2] Mojtaba Dehghan Manshadi [3*]

[1] *PhD. student, Faculty of Mechanical Engineering, Malek-Ashtar University of Technology; Iran, Isfahan. mqaed1100@gmail.com*
[2] *Assistant Professor, Faculty of Mechanical Engineering, Malek-Ashtar University of Technology; Iran, Isfahan. ehsanyari11@gmail.com*
[3] *Professor, Faculty of Mechanical Engineering, Malek-Ashtar University of Technology; Iran, Isfahan. dehghanmanshadi@gmail.com*

ARTICLE INFO

Article History:
Received: 23 May 2025
Last modification: 29 Jun 2025
Accepted: 8 Jul 2025
Available online: 9 Jul 2025

Article type:
Research Paper

Keywords:
Pre-swirl PumpJet, Duct Inlet Length, Stator-Rotor Distance, Hydrodynamic Performance, Open-Water Efficiency, Uncertainty Analysis

ABSTRACT

This study investigates the effect of duct inlet length on the hydrodynamic performance of a pre-swirl pump-jet system, focusing on open water efficiency through uncertainty analysis. To this end, five models with varying duct inlet lengths (0~0.1DRotor) were experimentally tested in the cavitation tunnel at Imam Khomeini Naval University in Noshahr. Sampled parameters included rotor thrust, combined duct and stator thrust, and rotor torque at eight advance ratios (J). Each measurement was repeated four times, and their averaged values were utilized in the calculations. Sensitivity analysis revealed that torque has a more significant impact on open-water efficiency compared to total thrust. Experimental test results demonstrated that the open water efficiency for all configurations reached a maximum at J=1.1. The L=0.1DR configuration exhibited the highest efficiency at 62.15%, representing a 5.15% improvement over the L=0DR configuration. The relative uncertainty of efficiency was below 5%, and the L=0.1DR configuration showed the smallest uncertainty range, indicating high experimental precision. Furthermore, an examination of the open water efficiency uncertainty range revealed that for advance ratios of 0.6, 1.1, and 1.4, the L=0.1DR configuration yielded the widest efficiency range. The upper bound of open water efficiency also belonged to the L=0.1DR configuration for other advance ratios. Therefore, based on the results of the conducted uncertainty analysis, the L=0.1DR configuration demonstrates improved open water efficiency performance compared to other configurations. This improvement is attributed to increased thrust resulting from better uniformity of the flow entering the stator and optimized angle of attack to the rotor blades.

DOI: http://dx.doi.org/10.61882/ijmt.21.1.54

1. Introduction

The demand for high-speed vessels in both military and commercial sectors has grown in recent decades. This has led to the design of marine propulsors with complex geometries, offering higher efficiency, reduced vibrations and noise, and more reliable operational capabilities. Podded propulsion systems, ducted propellers, and ducted systems are examples of successful designs in this area. Selecting the appropriate propulsion system is a crucial priority in the design process of vessels and submersibles. Years ago, the idea that increasing momentum could generate thrust led to the development of the first waterjet propulsion system. The history of using pump-jet propulsion systems for submarines and submersibles dates back several decades, but in recent years, pump-jet propulsion, especially for submarines, has gained significant attention. In 2018, at the request of the Australian Ministry of Defense, research was conducted to compare propeller propulsors and pump jets. The findings indicated that at high speeds and high advance ratios, the efficiency of pump-jet propulsors surpasses that of other propulsor types [1]. Pump-jets are primarily designed for submarines, where reduced noise and enhanced stealth are critical, thus justifying the use of this propulsor. Figure (1) illustrates a typical pump-jet propulsion system integrated into a hull within a cavitation tunnel.

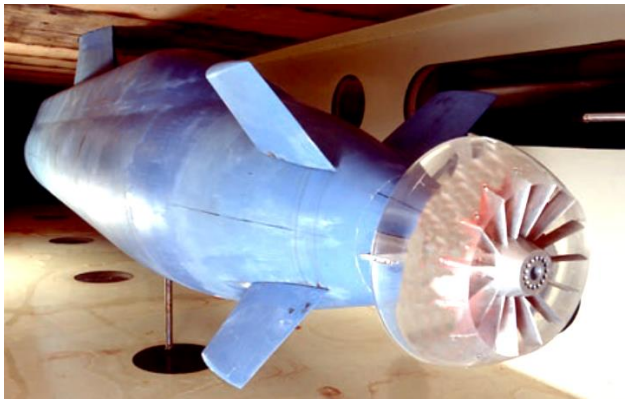

Figure 1. Pump jet on submarine model in the cavitation tunnel at SSPA [2]

In experiments where multiple factors influence a response variable, many tests are typically required across various configurations of the influential parameters. However, due to economic, time, and facility constraints, conducting tests in the desired quantity is often not feasible. Conversely, reducing the number of tests significantly compromises the accuracy of the results, sometimes rendering them unusable. Therefore, to reduce the number of tests and maintain the necessary accuracy, only those tests that are sufficiently impactful and whose results are generalizable should be selected and performed. The selection of these targeted and limited tests is achieved through the Design of Experiments (DOE) techniques, and the accuracy of the results is evaluated using Uncertainty Analysis. It is worth noting that the inherent nature of using targeted and designed experiments, by eliminating many unnecessary tests, intrinsically enhances the accuracy of the obtained results. Uncertainty analysis and DoE techniques emerged as a competitive approach in Western countries and Japan during the 1980s and 1990s [3]. Uncertainty is defined as the determination of the error range of a quantity, typically expressed with a 95% probability for engineering calculations [4]. Uncertainty analysis aims to determine each parameter's contribution to the total error of the quantity, which necessitates empirical data and testing. The proper application of DoE methods can facilitate the stages of designing and producing new products and improve existing outcomes. These principles are widely applied across various industries, including electronics and semiconductors, aerospace, automotive, medical equipment, food, pharmaceuticals, chemical, and process industries. Design of Experiments involves one or a series of experiments where deliberate changes are introduced to the process's input variables to observe and identify the resulting changes in the output response. As illustrated in Figure 2, a process can be conceived as a combination of equipment, methods, and personnel that transform input materials into an output product. This output product possesses one or more quality characteristics with observable responses. Some process variables, x1, x2…, xp, are controllable, while others, z1, z2…, zg, are uncontrollable (though they may be controllable under experimental conditions). In some cases, these uncontrollable factors are referred to as noise factors. The objectives of an experiment may include Identifying the variables (x) that have the most significant effect on the response (y), Determining the values of the variables (x) that most affect the response, such that y is close to its nominal value, Determining the values of the variables (x) that most affect the response, such that variations in y are minimized, Determining the values of the variables (x) that most affect the response, such that the effects of uncontrollable variables are minimized.

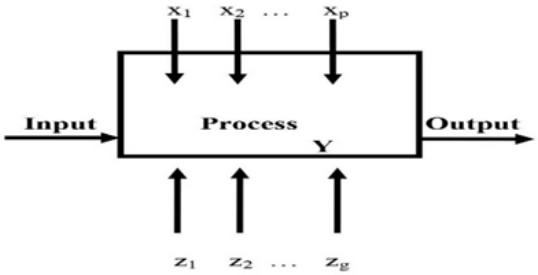

Figure 2. Illustrative Diagram of a Process [3]

The Design of Experiments (DOE) methodology can be employed to establish statistical process control and identify variables that influence a given process. A

straightforward application of uncertainty analysis and Design of Experiments techniques yields the following benefits: improved results, reduced variation and enhanced conformance to nominal values, decreased development time, and reduced costs. Furthermore, the Design of Experiments methodology can play a significant role in engineering design activities, including designing and developing existing products. [5]

2. Review of Recent Studies

Recent studies have explored various aspects of the hydrodynamic performance of pump jets and the associated uncertainties. A summary of key studies relevant to the topic is presented below: Qaedsharaf (2011) [۶], in his Master's thesis on heat transfer analysis and regression rate of solid fuel hybrid propellants using uncertainty analysis and curve fitting, obtained an empirical relationship for the heat transfer rate of hybrid propellants. Motallebi-Nejad et al. (2017) [7], though slightly older, is relevant due to its use of uncertainty analysis in CFD simulations for ducted propellers and pump jets. They employed the Grid Convergence Index (GCI) method to evaluate numerical errors, providing a framework for the present study. However, this study also did not address the duct inlet length. Using uncertainty analysis, Qaedsharaf et al. (2019) [۸] compared the performance and sensitivity of influential parameters in two propellants, oxygenated water and nitrous oxide. The results showed that using nitrous oxide propellant would be more desirable in accuracy, and its propulsive force would be closer to the desired propulsive force of 5 Newtons. Wang et al. (2019) [۹] examined the influence of duct geometric parameters on the hydrodynamic performance of a pump jet using a surface panel method. They analyzed parameters such as gap size, camber, and angle of attack, finding that these factors affect performance indicators, surface pressure distribution, and flow velocity. However, this study did not specifically address the duct inlet length or consider uncertainty analysis, indicating a need for more focused research. This study also did not include uncertainty analysis, which limits its ability to provide reliable results. Huang et al. (2020) [1۰] used advanced DES simulation to investigate the effects of duct parameters on the unsteady hydrodynamic performance of a pump jet. They showed that duct geometry influences thrust fluctuations and noise, but the duct inlet length was not explicitly examined. Chen et al. (2021) [1۱] combined CFD and experimental methods to investigate the effect of duct inlet length on the hydraulic performance of a waterjet propulsion device. They found that duct efficiency, head, and thrust peaked at an optimal length (L=1.12D), and flow uniformity improved with increasing length. Although this study focused on water jets, its findings are generalizable to pump jets; however, the absence of uncertainty analysis limited the accuracy of the results. Li et al. (2022) [12] comprehensively reviewed pump-jet hydrodynamic performance and design. They highlighted the importance of duct design in improving efficiency and reducing noise but did not address the duct inlet length. This study also did not mention uncertainty analysis, indicating a need for more rigorous approaches in future research. Zhou et al. (2023) [1۳] numerically analyzed the effects of duct profile parameters, such as camber and angle of attack, on the flow characteristics of a pump jet. They found these parameters affect flow uniformity and efficiency, indirectly linking to the duct inlet conditions. However, this study did not specifically investigate inlet length or consider uncertainty analysis. Zhou Qin Ji et al. (2024) [1۴] investigated the effect of rotor blade tip rake angle on the excitation force of a pump-jet propulsor in the same year. Their results demonstrate that the oscillation amplitude of the resulting horizontal (and vertical) forces acting on the duct/stator assembly significantly decreases with a reduced rake angle and increases with its increment. Dong Lin Xu et al. (2024). [۱۵] explored the relationship between longitudinal vibration size, frequency changes, excitation force, and the impact of vibration magnitude on the excitation force and vortex dynamic characteristics of a pump-jet propulsor. Ai Gan Wang et al. (2024) [۱۶] investigated the hydrodynamic noise characteristics of a pump-jet through both numerical and experimental methods. The results show that the amplitude of sound pressure level fluctuation in the radial plane exhibits an approximately circular distribution, and the sound pressure level also possesses characteristics of a dipole source. Li et al. (2024) [۱7] examined the hydrodynamic performance of a submarine equipped with a novel pump-jet propulsor. Their study noted that duct and stator configurations influence performance, though specific details regarding the inlet length or spacing were limited. Qaedsharaf et al. (2025) [۱۸] numerically investigated the cavitating performance of a pre-swirl pump-jet propulsion system by varying the chord length of the stator airfoil. Their findings indicate that increasing the stator chord length up to a certain point improves the propulsor's cavitating performance and reduces the likelihood of cavitation.

2.1. Identified Knowledge Gaps

Despite the advancements mentioned, several knowledge gaps were identified in the existing literature: Limited Focus on Duct Inlet Length: Most studies concentrate on general duct parameters like camber, angle of attack, or gap size. The duct inlet

length has not been specifically investigated, particularly in pre-swirl pump jets. Lack of Uncertainty Analysis: The use of uncertainty analysis in experimental pump-jet testing is minimal, which can compromise the accuracy and reliability of the results. Absence of Combined Studies: Few investigations have explored the combined effects of duct inlet length and other geometric parameters using experimental approaches and uncertainty analysis. Insufficient Focus on Pre-Swirl Pump-Jets: While some studies have addressed pump-jets, the specific flow dynamics have not been thoroughly examined.

2.2. Significance of the New Study

This study addresses existing knowledge gaps by systematically investigating the impact of the duct inlet length on the hydrodynamic performance of a pre-swirl pump-jet system and by employing uncertainty analysis to ensure the accuracy of the results. It provides reliable data that can offer precise design guidelines for optimizing duct geometry. The findings of this study have the potential to enhance hydrodynamic efficiency, which is crucial for underwater vehicles with stealth requirements and extended operational ranges. Furthermore, these findings can be applied to the design of other fluid machinery, such as turbines.

2.3. Conclusion

While the existing literature demonstrates significant advancements in understanding the hydrodynamic performance of pump jets, the specific influence of duct inlet length in pre-swirl pump jets and the application of uncertainty analysis remain underexplored. The present study contributes to scientific knowledge and practical applications in marine propulsion design by offering a comprehensive approach to bridge these gaps. By providing data-driven design guidelines, this research paves the way for developing more efficient and sustainable propulsion systems.

3. Theoretical Foundations and Governing Equations

3.1. Error in Experimental Studies

The topic of error is integral to various scientific and research endeavors, particularly in engineering and measurement sciences. The significance of knowing different quantities and understanding the sources that generate and propagate errors is universally acknowledged. Therefore, it is essential to address error analysis and uncertainty, understand error propagation, identify the impact of parameter errors on the main result, and control them to achieve the desired engineering precision. The presence of error indicates the discrepancy between a measurement and its actual or standard value (with much higher accuracy than typical measurements). Error leads to deviations from the desired outcome, and if left uncontrolled, the project may stray from its objectives and mission. This control must be enough to meet design requirements, as exceeding this incurs additional time and cost. Since errors cannot be eliminated from any process, the goal is to minimize them while considering the maximum required accuracy. Uncertainty analysis identifies error sources, quantifies the error from each source, and offers strategies to reduce errors in key parameters. In error analysis, one must assess the source of error generation and propagation and its impact on the final uncertainty. The level of final uncertainty is estimated based on the uncertainty in the measured input parameters.

Assuming that human errors or general errors are not relevant (i.e., they either do not exist or can be corrected), the primary errors are categorized into three main, examinable types: conceptual, systematic, and random errors [5].Conceptual Error: Conceptual errors refer to those arising from inherent measurement inaccuracies, flaws in the measurement method, inability to access the actual values of quantities, errors in the standards themselves, underlying assumptions and initial hypotheses governing the problem, avoidance of mathematical complexities, simplification of relationships, and linear assumptions for variations, among others. These are typically irreducible. In this study, the following factors can introduce conceptual errors: Mathematical Model Simplification: The governing equations for pump-jet hydrodynamic performance (such as reduced efficiency equations) are based on steady and uniform flow assumptions. These simplifications might not accurately capture unsteady flow dynamics, like vortices or instability effects. Lack of Modeling for Tunnel Wall and Wake Region Effects: Experiments were conducted in a cavitation tunnel, a controlled environment that does not account for real-world effects like the interaction of tunnel walls and the wake region with the propulsor. This assumption can lead to errors when generalizing results to real-world conditions. Assumption of Parameter Independence: The reduced equation assumes that input parameters (like thrust and torque) are somewhat independent, whereas, in reality, these parameters might influence each other non-linearly. Systematic Error: Systematic errors constitute a significant and broad portion of the total error. They primarily originate from measurement equipment, calibration, and experimental methods. In this study, these errors were controlled mainly through the use of precise instruments and repeated experiments, and they were mostly minimized during the calibration process. Indeed, the calibration process is a form of correction and error control in the measuring device with very high precision standards. However, the following factors can still introduce systematic errors: Measurement Equipment Accuracy:

Load Cells: Load cells were used to measure the thrust of the duct-stator and rotor assembly. Any error in load cell calibration or their sensitivity to environmental conditions (such as temperature or tunnel vibrations) can lead to errors in thrust data. Torque Dynamometer: The rotor torque was measured separately. The dynamometer's accuracy and the impact of friction or misalignment of the drive shaft can introduce errors. Speed and Advance ratio Setting: Tunnel equipment sets the rotational speed (n=27.8 revolutions per second) and advance speed. Any deviation in the calibration of this equipment can affect the results. Geometry Manufacturing: Test models were fabricated using a 3D printer with 1-micron precision.

However, any surface roughness, dimensional deviation, or differences in material properties (like composites) can affect the flow and, consequently, the results. Equipment Installation and Alignment: Models were installed in the cavitation tunnel using an airfoil strut and a tongue. Any misalignment in the installation or the hydrodynamic effect of the strut on the flow can lead to measurement errors. Random Error: Random errors arise from unpredictable variations in the measurement process and are reduced by repeated experiments. They have no specific source and take on different values with each measurement. In this study, using Cochran's formula and repeating measurements four times helped reduce these errors. However, the following factors can still introduce random errors: Environmental Condition Changes: Cavitation Tunnel Temperature and Pressure: Variations in water temperature or pressure in the tunnel can affect fluid density and viscosity, influencing thrust and torque coefficients. Flow Fluctuations: Any fluctuations in the tunnel's inlet flow (such as turbulence or vibrations) can cause random variations in thrust and torque data. Operator Error: While operator training can reduce human errors, slight differences in measurement methods or data recording by different individuals can introduce random errors. Limited Number of Replications: Although four replications were performed for each measurement, the limited number of samples might not fully capture all random variations, especially at advance ratios with higher uncertainty.

3.2. Sensitivity Analysis

The influence of parameters and their errors on the function varies and requires case-by-case examination. It is impossible to identify a specific parameter as influential simply because its value is larger or has higher power than others before calculating and estimating its error. Instead, one must always first use sensitivity analysis, then determine the uncertainty error for each parameter, and then judge the determinative extent of each by relative comparison with other parameters. Increasing the number of measurements enhances the accuracy of the uncertainty determination process.

Identifying error sources from the sensitivity analysis equations for each parameter is straightforward. In other words, if quantity A is a function of 'n' independent parameters, such that the maximum possible and utilized accuracy in measuring each parameter is represented as Δn, then applying the error of each parameter in the function relationship for A will result in a change in the value of quantity A. If this change is greater for one parameter's error than others, that parameter is considered the primary source of error. This analysis continues down to the smallest error source. Generally, parameters with larger powers, larger error magnitudes, larger coefficients, and parameters present in multiple terms of the function equation are usually among those with high influence. On the other hand, we know well that constants like the gravitational or universal gas constant, etc., and specific numbers like pi or Napier's number, etc., are sufficiently accurate in calculations because they are computed and available to several hundred decimal places. Their error can be neglected compared to the error of other parameters. Sensitivity analysis is determined by partially differentiating the reduced equation and substituting a data set.

3.3. Uncertainty Analysis

The actual value of an object is never perfectly known. Any measuring instrument can only indicate its value to the extent of its precision. Therefore, there is always an unavoidable error in measurements and calculations unless a specific accuracy limit is desired. Since no measurement is immune to error, in any laboratory process, considering the inherent measurement errors, uncertainty analysis is undertaken to determine the required precision of the results or the extent to which the obtained results possess the necessary certainty. Through relevant techniques, the aim is first to determine the amount of uncertainty and then, based on an analysis of its error and available resources, to reduce it. Uncertainty involves defining the margin of error and determining each parameter's contribution to the total error. Addressing uncertainty requires empirical data and testing. The first step in uncertainty analysis is always to arrive at a relationship or function that is, firstly, very comprehensive, meaning it includes all possible and influential parameters. Secondly, its parameters are defined independently and are certainly measurable. This equation is referred to as the data reduction equation.

3.4. Strategies for Error Reduction

Key strategies for reducing error include increasing measurement accuracy, utilizing multiple types of equipment and measurement methods with very high standards, calibrating measuring devices, repeating

measurements, correctly applying statistical methods and models, excluding outliers (data points very far from the mean) provided it is confirmed that the outlier is due to a gross measurement error, maintaining precision in the decimal places of numbers in calculations according to the required accuracy, using sufficient memory for storing numbers in computer programs and training the person performing the measurements. As observed, implementing all these strategies requires significant time and cost. Therefore, it is wiser to identify the sources of error (parameters) with higher impact and concentrate on controlling their precision [5]. It is worth noting that the total error is a function of the error from using the measuring instrument (like calibration) and the error resulting from the data reduction equation. Depending on the magnitude of a parameter, the precision of the measuring device, and the type of governing equation, the influence of parameters and their error on the function is variable and requires case-by-case examination. One cannot necessarily identify a specific parameter as influential simply because its value is greater than other parameters or it has a higher power before calculation and error estimation. Instead, one must always first use sensitivity analysis and then determine each parameter's error (uncertainty), and then, by relative comparison with other parameters, judge the determinative extent of each.

3.5. Governing Equations

The first step in calculating uncertainty is forming the reduced equation. Before explaining this, the functional parameters of a jet pump must be defined. The following dimensionless coefficients are defined to analyze the hydrodynamic performance of a jet pump propulsion system. In marine references, dimensionless parameters such as thrust coefficient, torque coefficient, advance ratio, and open-water efficiency have been defined and used to compare the performance of propellers. The resultant horizontal force on the rotor, stator, and duct is considered the thrust force, and the rotor's driving torque is considered the propeller torque in these relationships. These dimensionless parameters are as follows [19, 20]:

$$\begin{cases} J = \frac{V_A}{nD} \quad K_{TR} = \frac{T_R}{\rho n^2 D^4} \quad K_{TS} = \frac{T_s}{\rho n^2 D^4} \quad K_{TD} = \frac{T_D}{\rho n^2 D^4} \\ K_{QR} = \frac{Q_R}{\rho n^2 D^5} \quad K_Q = K_{QR} \quad K_T = K_{TR} + K_{TS} + K_{TD} \\ \eta_o = \frac{JK_T}{2\pi K_Q} \end{cases} \quad (1)$$

Where J is advance ratio, K_T is total thrust coefficient, K_{TR} is rotor thrust coefficient, K_{TS} is stator thrust coefficient, K_{TD} is duct thrust coefficient, K_Q is torque coefficient, K_{QR} is rotor torque coefficient, η_o is open-water propeller efficiency, D is propeller diameter (m), n is rotational speed (rps), V_A is advance velocity (m/s), ρ is water density(kg/m^3). If we calculate the open water efficiencyη_o from the above relationships, we will have:

$$\eta_o = \frac{JK_T}{2\pi K_Q} = \frac{V_A(T_R + T_D + T_S)}{2\pi nQ} = \frac{V_A T_{Tot}}{2\pi nQ} \quad (2)$$

The total thrust is the sum of the rotor, duct, and stator thrusts. In the conducted experimental test, the thrust of the duct and stator assembly was sampled multiple times together, while the rotor thrust and torque were sampled separately. These values are then substituted into the relationships after averaging multiple sampling instances. Let's assume the quantity η_o is the primary quantity, which is a function of the independent parameter J:

$$\eta_o = f(X_1.X_2.\ldots X_J) = f(V_A.T_{Tot}.n.Q) \quad (3)$$

Accordingly, the reduced equation will be:

$$\eta_o = \frac{V_A T_{Tot}}{2\pi nQ} \quad (4)$$

The sensitivity of η_o to the results of each of these parameters is then obtained by substituting the results into the following relationship [5]:

$$Sensitivity = \left(\frac{\partial \eta_o}{\partial X_i}\right) \quad (5)$$

The uncertainty of η_o arises from the uncertainty of the effective input values (X_i) on the governing equation, or the error of each parameter (U_{X_i}) [5]:

$$U_{\eta_o} = \sqrt{\sum_{i=1}^{n} \left(\frac{\partial \eta_o}{\partial X_i} U_{X_i}\right)^2} \quad ; U - U_{\eta_o} \le U_t \le U + U_{\eta_o} \quad (6)$$

In the error analysis process, after determining the uncertainty value of each parameter (U_X), which is obtained from measurements, and by using statistical relationships and sensitivity analysis of the governing equation, the amount of uncertainty in the primary quantity (U_{η_o}) is determined. It can then be stated that the true value (U_t) lies within the obtained range. The smaller the value of Uηo, the higher the certainty in the quantity η_o (the obtained range will be smaller), and it approaches a more reliable value. It can be concluded that the total uncertainty results from the uncertainty in each parameter, and by reducing the uncertainty in the parameters, the certainty in the value of that quantity can be increased. Therefore, the uncertainty for the function η_o represents the dependency of the function η_o on parameter x and the error present in that parameter (RSS) [5]:

$$U_{\eta_o}^2 = (\frac{\partial \eta_o}{\partial X_1})^2 U_{X_1}^2 + (\frac{\partial \eta_o}{\partial X_2})^2 U_{X_2}^2 + \cdots + (\frac{\partial \eta_o}{\partial X_J})^2 U_{X_J}^2 \quad (7)$$

Now, if the relative uncertainty is considered [5]:

$$\frac{U_{\eta_o}^2}{\eta_o^2} = (\frac{X_1}{\eta_o}\frac{\partial \eta_o}{\partial X_1})^2 (\frac{U_{X_1}}{X_1})^2 + (\frac{X_2}{\eta_o}\frac{\partial \eta_o}{\partial X_2})^2 (\frac{U_{X_2}}{X_2})^2 + \cdots + (\frac{X_J}{\eta_o}\frac{\partial \eta_o}{\partial X_J})^2 (\frac{U_{X_J}}{X_J})^2 \quad (8)$$

In the latter relationship, other parameters can be replaced with the open water efficiency. Relative uncertainty is often expressed as a percentage. The measurable parameters in the conducted experimental test include: rotor thrust, rotor torque, and the thrust of the duct and stator assembly. The value of n is a constant 27.8 revolutions per second, and V_A is adjusted depending on the advance ratio via tunnel equipment, which has been previously calibrated and verified by a qualified company. To calculate the values of total uncertainty, relative uncertainty, and sensitivity analysis, relevant relationships were programmed in MATLAB software, and the corresponding results were extracted. In this study, uncertainty analysis was conducted based on the classical approach to measurement uncertainty, which is also endorsed by reputable engineering standards such as ASME PTC 19.1 and international guidelines.

4. Experimental Investigation

To investigate the effect of the duct inlet region and the gap between the rotor and stator on the hydrodynamic performance of the propulsion system, five models were designed. These models varied the inlet length L by displacing the stator from the duct inlet opening towards the rotor. The tested inlet lengths were L=0DR, L=0.025DR, L=0.050DR, L=0.075DR, and L=0.1DR, where DR denotes the rotor diameter. Each model was individually tested in a cavitation tunnel. The components of the pre-swirl jet pump are also visible in Figure 3.

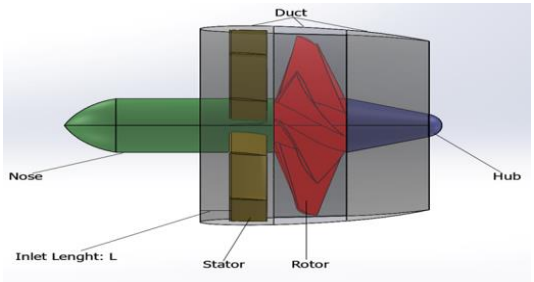

Figure 3: Component Diagram of the Pre-swirl Jet Pump

Experimental testing was conducted in the cavitation tunnel at Imam Khomeini Naval University (Noshahr) (Figure 4).

Figure 4: View of the Cavitation Tunnel at Imam Khomeini Naval University (Noshahr)

To install the geometry within the cavitation tunnel, an airfoil-shaped support base was affixed beneath the designed geometries. This base included a tab for measuring the thrust of the combined duct and stator assembly via a load cell. The geometries themselves were fabricated using a 3D printer with composite materials, achieving a precision of 1 micron. Figure 5 illustrates the five geometries manufactured for these experimental tests. Table 1 presents the geometric specifications of the designed propulsion system.

Figure 5: Five Geometries Fabricated for Experimental Testing

Table 1. Geometric specifications of the pump jet propulsion system

Characteristic	Value
Rotor diameter (cm)	9
Number of rotor blades and their profile	7 - NACA16
Number of stator blades and their profile	11 - NACA66
Duct type and its profile	Convergent - NACA6608
Inlet diameter, outlet diameter and duct length (cm)	12.05,9.12and١٣,٠٦

The load cell and the propeller holding mechanism were secured within the tunnel using three weights. The rotor was separately mounted onto a drive shaft, which was connected to the thrust and torque measurement equipment. Figure 6 displays a schematic of the cavitation tunnel with the installed propeller assembly.

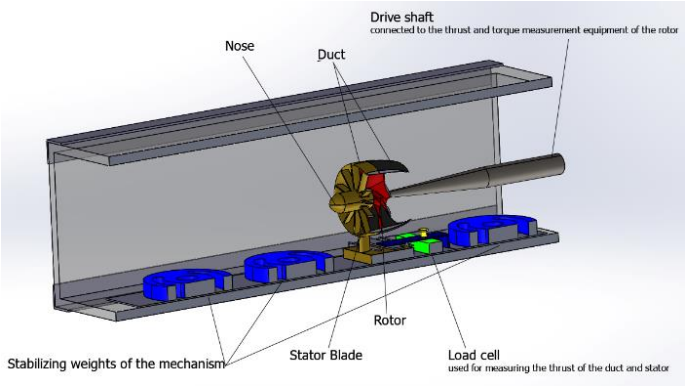

Figure 6: Installation Method of the Propeller Assembly in the Cavitation Tunnel

Three parameters were measured: rotor thrust, duct and stator thrust, and rotor torque. The experimental tests following standard laboratory procedures in the field of hydrodynamics. To determine the minimum number of repetitions for each data acquisition, Cochran's Sample Size Formula was employed, which is one of the most reliable and widely used statistical methods for sample size determination in scientific experiments. Introduced by William Cochran in 1931, Cochran's formula is a widely used and crucial method for calculating statistical sample sizes. It assumes a normal distribution of data for determining the number of repetitions. This formula facilitates the estimation of sample size for forming a statistical population. It is typically used in two scenarios: when the population size is known and when it is unknown. For a known population size, Cochran's formula is applied as follows:

$$n = \frac{\frac{pqz^2}{d^2}}{1+\frac{1}{N}\left[\frac{z^2pq}{d^2}-1\right]} \qquad (9)$$

In this formula, if the values of 'p' and 'q' are unknown, their maximum value of 0.5 is used. Additionally, the statistic 'z' can be interchangeably used with 't'. At a 5% error level, the value of 'z' is 1.96, and z2 is 3.8416. Furthermore, given that sampling accuracy depends on the margin of error (confidence interval 'd'), the maximum 'd' value of 5% is utilized if the researcher aims for maximum sampling accuracy. Substituting these values yields a minimum sample size of 2.9844623990055936. Four repetitions were set for each data acquisition session to ensure greater accuracy. Subsequently, eight advance ratios were considered, and for each ratio, data for the three aforementioned parameters were collected in four repetitions. The average of these measurements was then used in the relevant calculations.

5.1. Sensitivity Analysis

Using Equation 5 from the previous section and substituting the values sampled during an initial series of experimental tests, a sensitivity analysis was performed for five designed geometries concerning rotor torque and total thrust. The results are presented in Figure 7. An examination of the graph reveals that torque demonstrates greater sensitivity to the free water efficiency results for most advance ratios across all five designed geometries. This observation can be justified by examining both the reduced equation and the differential sensitivity relationship, as torque appears in the denominator of the fractional reduced equation. The interpretation of these results indicates that greater precision is required in data collection for the rotor torque parameter.

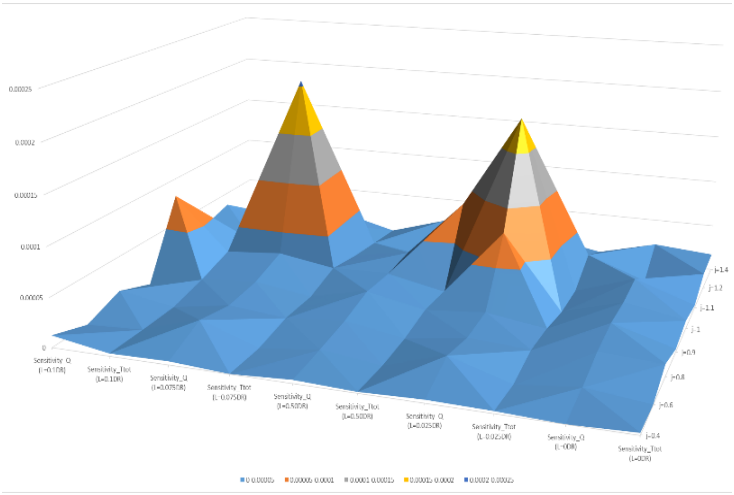

Figure 7: Comparative Analysis of Open Water Efficiency Sensitivity to Rotor Torque and Total Thrust

5.2. Case 1: L=0DR (Stator at Duct Inlet)

In this configuration, the inlet region length (L) is considered zero, with the stator positioned at the entrance of the duct. Based on the experimental test results shown in Figure 8, the following maximum values were observed at various advance ratios: Maximum efficiency: 59.12% at an advance ratio of 1.1, Maximum thrust coefficient: 0.4765, Maximum torque coefficient: 0. 09651. The thrust coefficient generally exhibits a nearly decreasing trend with an increasing advance ratio. The open-water efficiency curve shows a completely ascending trend up to an advance ratio (J) of 1.1, after which it follows a fully descending trend. The uncertainty values for open-water efficiency are presented in Figure 8. The highest open-water efficiency uncertainty, at 0.006254, occurred at an advance ratio of 1.4, while the lowest, at 0.001491, was observed at an advance ratio of 0.4. Considering this uncertainty, the maximum open-water efficiency at an advance ratio of 1.1 falls within the range of 0.586183 to 0.596217. Figure 8 also displays

the open-water efficiency for all advance ratios and their upper and lower bounds. Figure 8 illustrates the relative uncertainty percentage for various parameters, including stator duct thrust, rotor thrust, total thrust, rotor torque, and open-water efficiency. The graph shows that the maximum relative uncertainty belongs to open-water efficiency, at 1.784863%. This value is less than 5%, indicating the high precision of the conducted experiments.

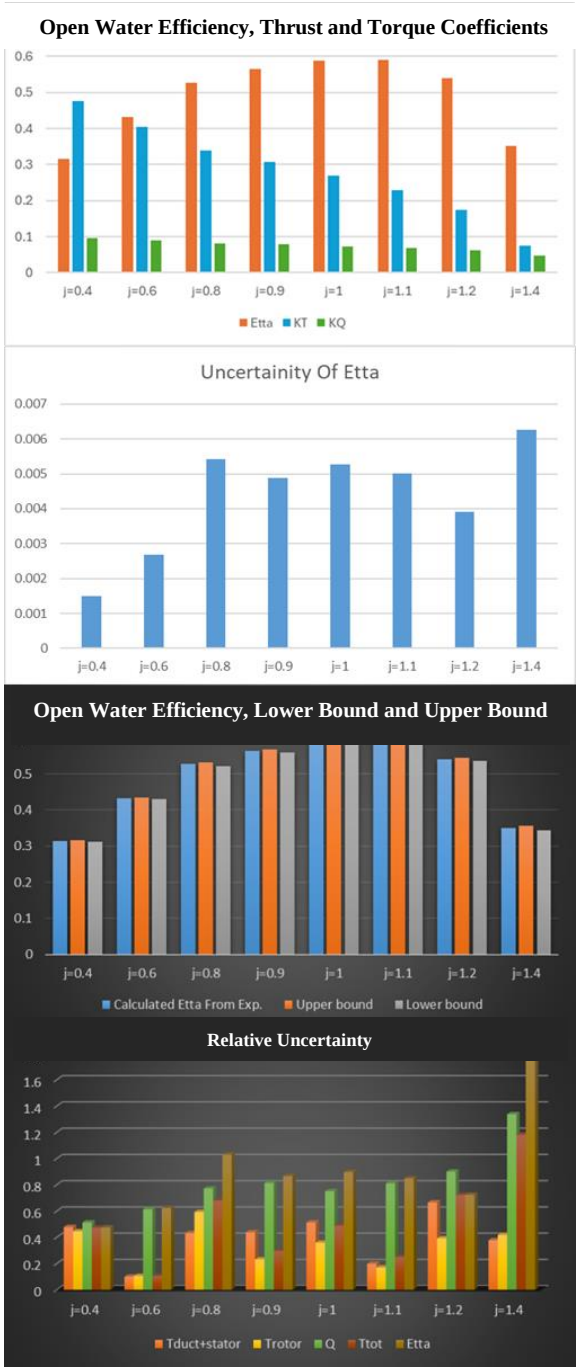

Figure 8: Bar chart arrangement. Up to down: Efficiency plot, thrust and torque coefficients, open water efficiency uncertainty plot, Open water efficiency values with upper and lower bounds; relative uncertainty plot for duct and stator thrust, rotor thrust, total thrust, rotor torque, and open-water efficiency parameters (in percentage terms) across different advance ratios for the L=0DR configuration.

5.3. Case 2: L=0.025DR

In this case, the inlet section length is set to 0.00225 meters. Based on this, for various advance ratios, the maximum open-water efficiency is 59.51% at an advance ratio of 1.1. The maximum thrust coefficient is 0.4887, and the maximum torque coefficient is 0.09723. Similar to the previous case, the open-water efficiency curve shows a completely increasing trend up to an advance ratio of J=1.1, and a distinctly decreasing trend thereafter. The thrust coefficient and torque coefficient curves generally exhibit a decreasing trend with increasing advance ratio, apart from minor fluctuations. The results are presented in Figure 9. The uncertainty values for open-water efficiency are also shown in Figure 9. The highest uncertainty in open-water efficiency is 0.008929 at an advance ratio of 1, while the lowest is 0.002345 at an advance ratio of 0.4. Considering the maximum uncertainty in open-water efficiency, the value at an advance ratio of 1.1 falls within the range of 0.584771 to 0.603724. Figure 9 illustrates the open-water efficiency for all advance ratios, along with their upper and lower bounds.

The relative uncertainty percentages for the parameters including stator duct thrust, rotor thrust, total thrust, rotor torque, and open-water efficiency are also presented in Figure 9. As is evident from the plot, the maximum relative uncertainty is associated with the open-water efficiency, at 1.689285%. This value is less than 5%, indicating the high accuracy of the conducted experiments.

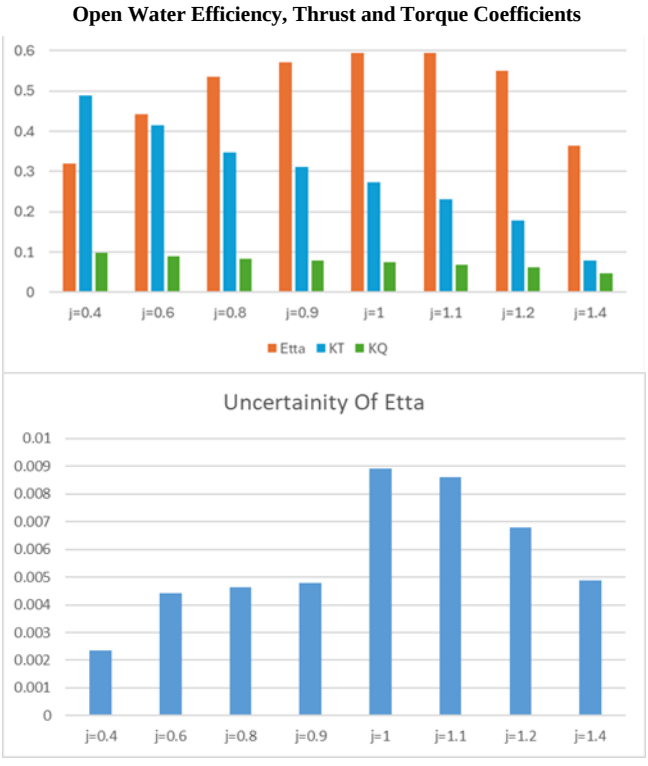

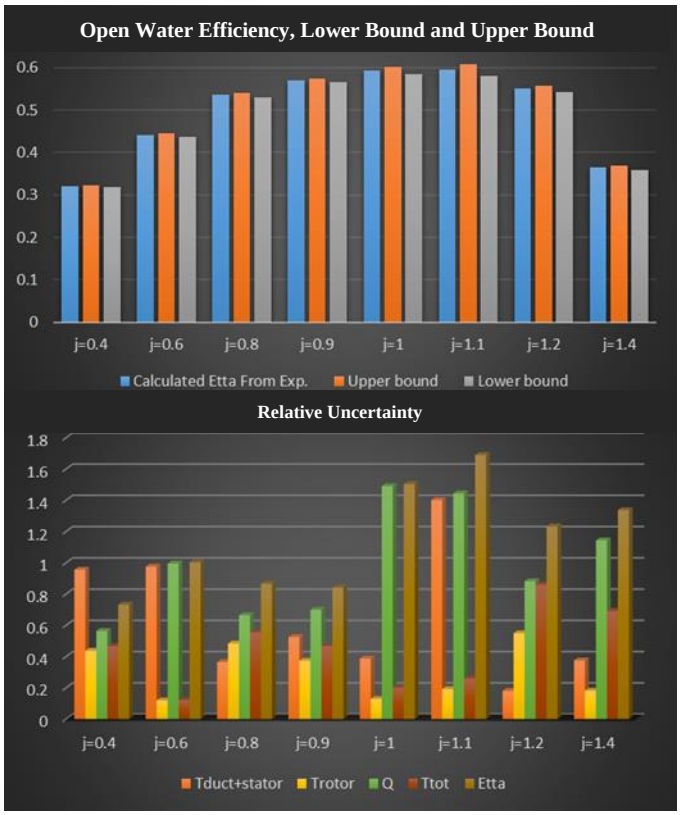

Figure 9: Bar chart arrangement. Up to down: Efficiency plot, thrust and torque coefficients, open water efficiency uncertainty plot, Open water efficiency values with upper and lower bounds; relative uncertainty plot for duct and stator thrust, rotor thrust, total thrust, rotor torque, and open-water efficiency parameters (in percentage terms) across different advance ratios for the L=0.025DR configuration.

5.3. Case 2: L=0.025DR

In this case, the inlet section length is set to 0.00225 meters. Based on this, the maximum open-water efficiency for various advance ratios is 59.51% at an advance ratio of 1.1. The maximum thrust coefficient is 0.4887, and the maximum torque coefficient is 0.09723. Like the previous case, the open-water efficiency curve shows a completely increasing trend up to an advance ratio of J=1.1 and a distinctly decreasing trend thereafter. The thrust coefficient and torque coefficient curves generally exhibit a decreasing trend with increasing advance ratio, apart from minor fluctuations. The results are presented in Figure 9. The uncertainty values for open-water efficiency are also shown in Figure 9. The highest uncertainty in open-water efficiency is 0.008929 at an advance ratio of 1, while the lowest is 0.002345 at an advance ratio of 0.4. Considering the maximum uncertainty in open-water efficiency, the value at an advance ratio of 1.1 falls within the range of 0.584771 to 0.603724. Figure 9 illustrates the open-water efficiency for all advance ratios and their upper and lower bounds.

Figure 9 also presents the relative uncertainty percentages for the parameters, including stator duct thrust, rotor thrust, total thrust, rotor torque, and open-water efficiency. As the plot shows, the maximum relative uncertainty is associated with the open-water efficiency, at 1.689285%. This value is less than 5%, indicating the high accuracy of the experiments that were conducted.

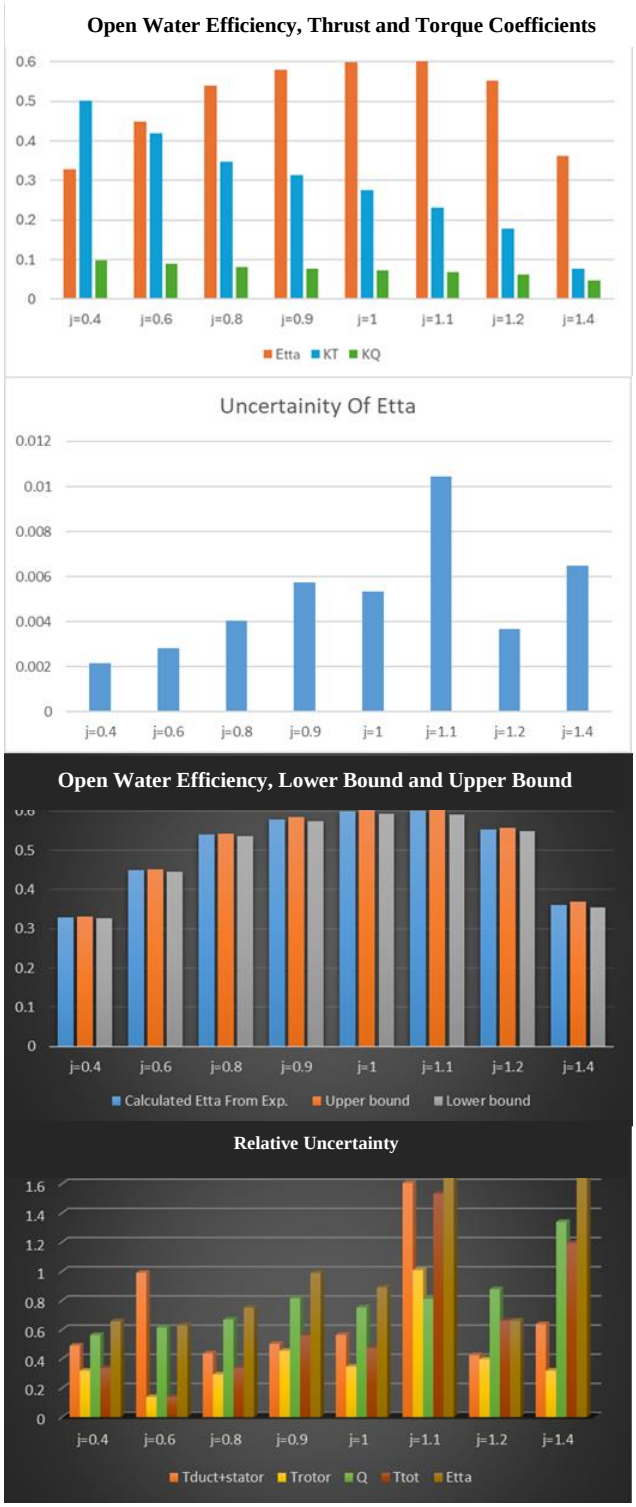

Figure 10: Bar chart arrangement. Up to down: Efficiency plot, thrust and torque coefficients, open water efficiency uncertainty plot, Open water efficiency values with upper and lower bounds; relative uncertainty plot for duct and stator thrust, rotor thrust, total thrust, rotor torque, and open-water efficiency parameters (in percentage terms) across different advance ratios for the L=0.050DR configuration.

5.5. Case 4: L = 0.075DR

In this case, the length of the inlet section was considered 0.00675 meters. Based on this, at various advance ratios, the maximum efficiency is 0.6105 at an advance ratio of 1.1, the maximum thrust coefficient is 0.4761, and the maximum torque coefficient is 0.09353. Similar to previous cases, the efficiency plot shows a completely increasing trend up to an advance ratio of J=1.1, after which it exhibits a completely decreasing trend. The thrust coefficient plot shows an approximately decreasing trend. The torque coefficient also behaves similarly to the previous case. The results are visible in Figure 11. The highest open water efficiency uncertainty occurs at an advance ratio of 1 with a value of 0.006943, and the lowest uncertainty is at an advance ratio of 0.4 with a value of 0.00191. Considering the maximum open water efficiency uncertainty at an advance ratio of 1.1, the value falls within the range of 0.606408 to 0. 614592. Figure 11 presents all advance ratios' open water efficiency and upper and lower bounds. Furthermore, Figure 11 displays the relative uncertainty values in percentage for stator duct thrust, rotor thrust, total thrust, rotor torque, and open water efficiency. As the plot indicates, the maximum relative uncertainty pertains to the open water efficiency, standing at 1.422993%, which is less than 5%, demonstrating the high accuracy of the conducted experiments.

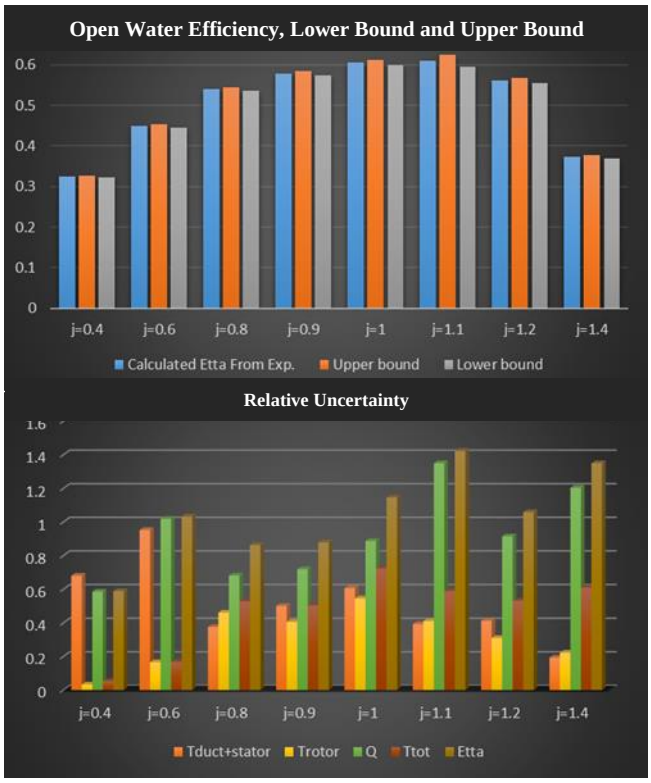

Figure 11: Bar chart arrangement. Up to down: Efficiency plot, thrust and torque coefficients, open water efficiency uncertainty plot, Open water efficiency values with upper and lower bounds; relative uncertainty plot for duct and stator thrust, rotor thrust, total thrust, rotor torque, and open-water efficiency parameters (in percentage terms) across different advance ratios for the L=0.075DR configuration.

5.6. Case 5: L=0.1DR

In this case, the inlet length was set to 0.009 meters. Based on this, at various advance ratios, the maximum efficiency was 0.62 at an advance ratio of 1.1, the maximum thrust coefficient was 0.5117, and the maximum torque coefficient was 0.0989. Like previous cases, the open water efficiency plot shows a completely increasing trend up to J=1.1 and a completely decreasing trend from this advance ratio onwards. The highest efficiency among all investigated cases is observed in this condition. The results are presented in Figure 12. The maximum open water efficiency uncertainty is 0.010235 at an advance ratio of 1, and the minimum is 0.001685 at an advance ratio of 0.6. Considering the maximum open water efficiency uncertainty at an advance ratio of 1.1, the value falls within the range of 0.61741 to 0.62559. Figure 12 illustrates the open water efficiency for all advance ratios and their upper and lower bounds. The chart in Figure 12 also presents the relative uncertainty values for stator duct thrust, rotor thrust, total thrust, rotor torque, and open water efficiency (in percentage). The chart shows that the maximum relative uncertainty is related to the open water efficiency at 1.663996%. This value is less than 5%, indicating the high precision of the experiments conducted.

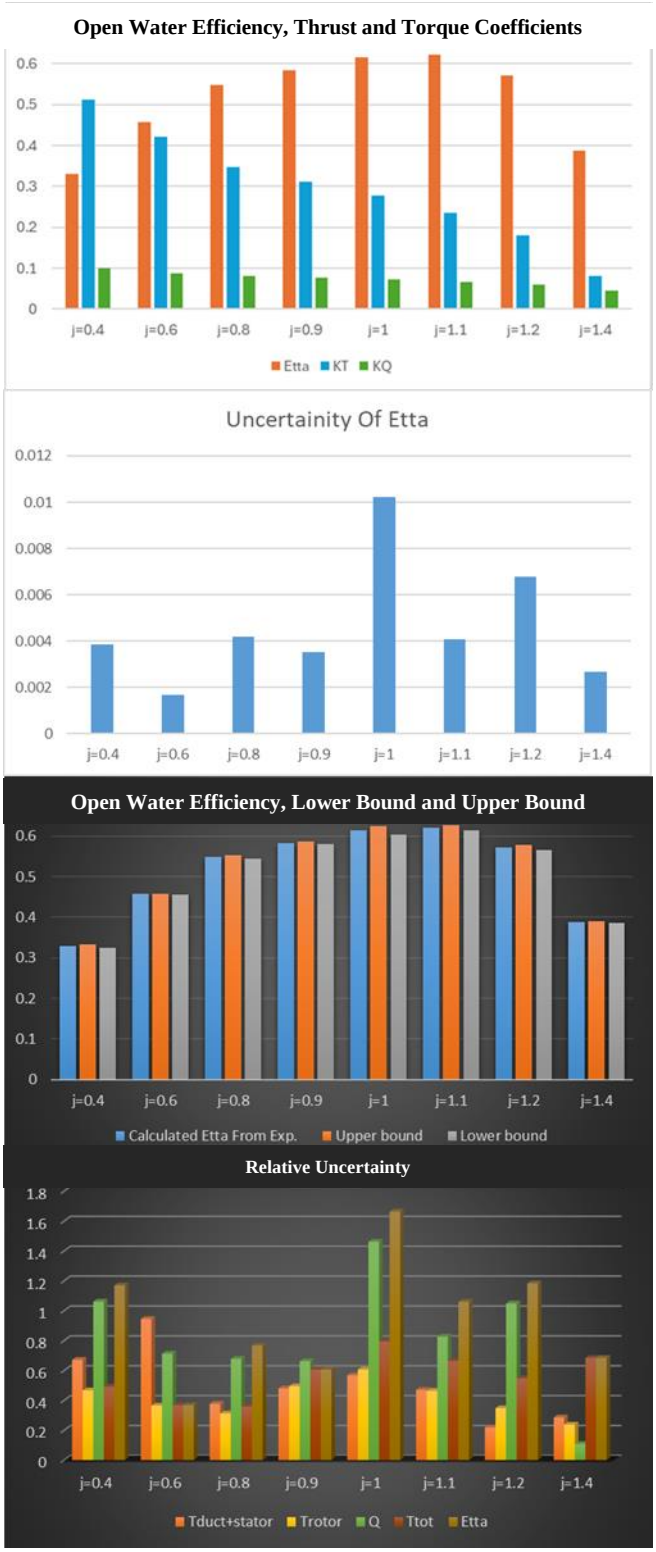

Figure 12: Bar chart arrangement. Up to down: Efficiency plot, thrust and torque coefficients, open water efficiency uncertainty plot, Open water efficiency values with upper and lower bounds; relative uncertainty plot for duct and stator thrust, rotor thrust, total thrust, rotor torque, and open-water efficiency parameters (in percentage terms) across different advance ratios for the L=0.01DR configuration.

6. Discussion of Results

6.1. Relative Uncertainty

The relative uncertainty values for the stator-duct assembly thrust, rotor thrust, and total thrust are presented in Figure 13. The relative uncertainty of the stator-duct assembly thrust varies from 0.1001% (L=0DR, J=0.6) to 1.605497% (L=0.050DR, J=1.1). Similarly, the relative uncertainty of the rotor thrust ranges from 0.033333% (L=0.075DR, J=0.4) to 1.007751% (L=0.050DR, J=1.1). The relative uncertainty of the total thrust varies from 0.054456224% (L=0.075DR, J=0.4) to 1.533078% (L=0.050DR, J=1.1). Figure 13 also shows the relative uncertainty values for rotor torque and open water efficiency. The rotor torque uncertainty ranges from 0.1087% (L=0.1DR, J=1.4) to 1.490312966% (L=0.025DR, J=1). The relative uncertainty of the open water efficiency varies from 0.368471123% (L=0.1DR, J=0.6) to 1.794043915% (L=0.050DR, J=1.4). Based on these findings, the maximum relative uncertainty among all these parameters is 1.794043915% (L=0.050DR, J=1.4). This value is considered desirable for engineering calculations and indicates the high accuracy of the experimental test conducted [5].

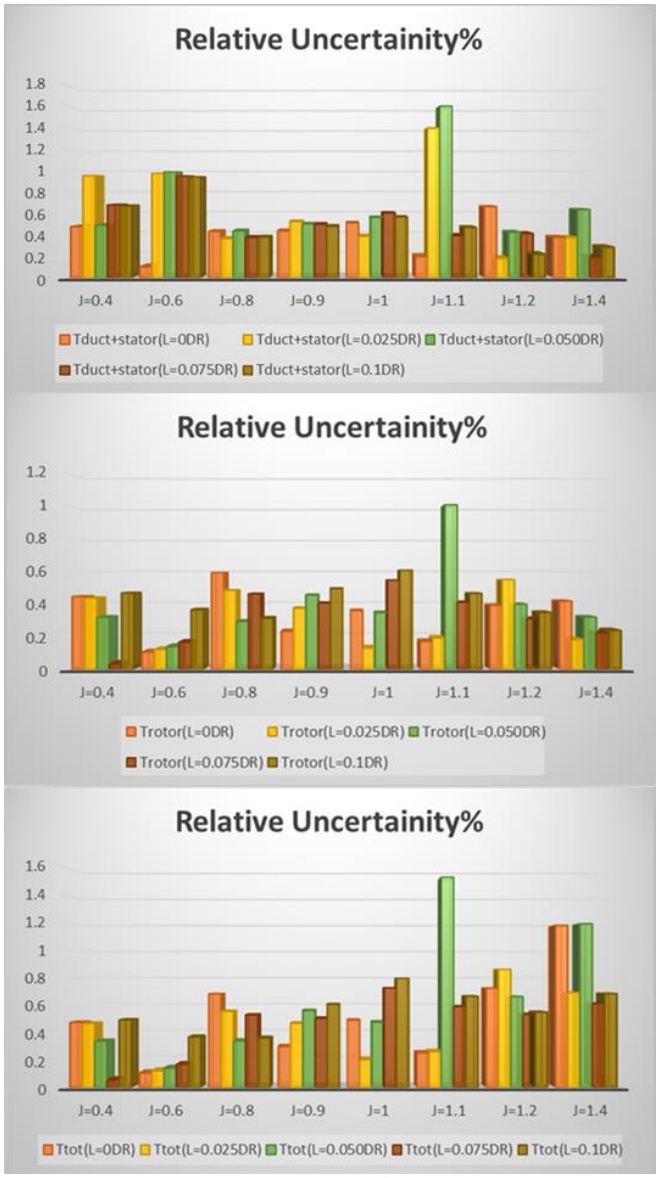

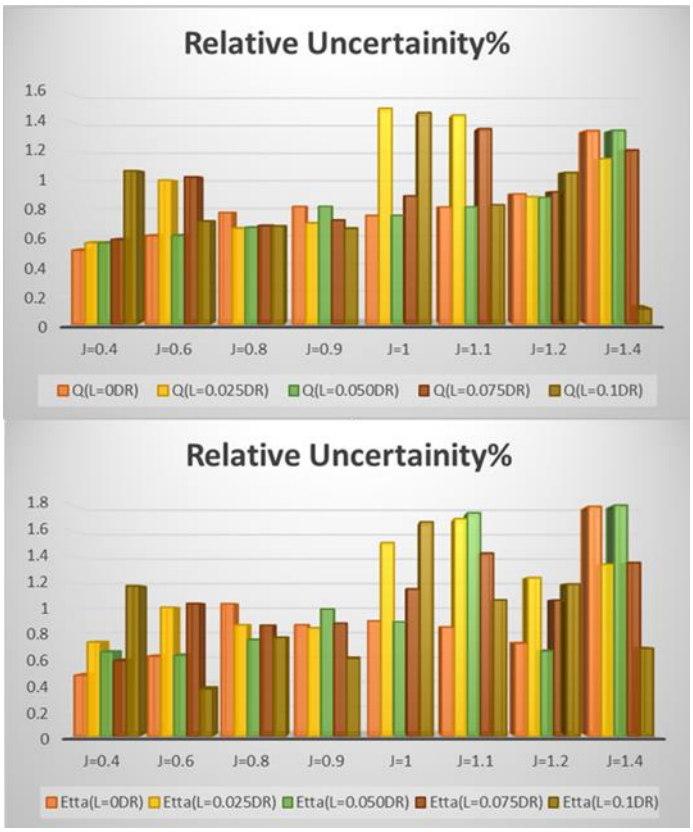

Figure 13: Comparative Bar Chart of the Percentage Relative Uncertainty for Duct and Stator Assembly Thrust, Rotor Thrust, Total Thrust, Rotor Torque, and Open waterEfficiency for Five Investigated Conditions at Various Advance ratios.

6.2. Total Thrust Coefficient

Referring to the comparative diagram in Figure 14, the L=0.1DR condition exhibits the highest thrust coefficient across the most advance ratios. Minor differences are observed only within the range of J=1.1 to J=1.4 compared to other conditions. In the remaining conditions, discrepancies are noticeable within J=0.4 to J=0.8 and J=1.1 to J=1.4, while no significant differences are observed in other ranges. The trend for all conditions is decreasing from J=0.4 to J=0.6, then increasing from J=0.6 to J=0.8, and thereafter solely decreasing.

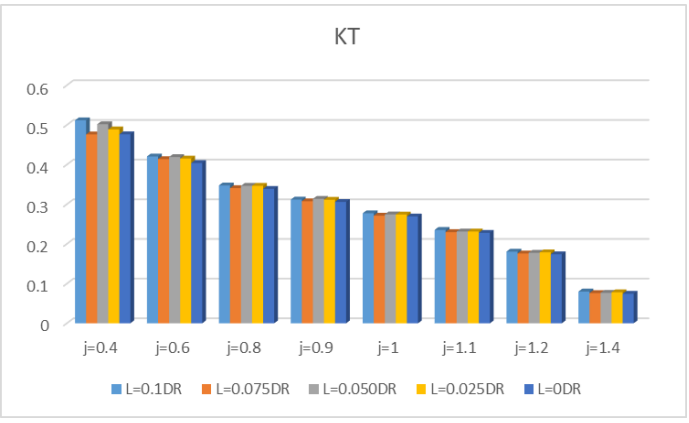

Figure 14: Comparative Bar Chart of Total Thrust Coefficient for Five Investigated Cases at Various Advance ratios

6.3. Torque Coefficient

A close examination of Figure 15 reveals that the L=0.025DR condition exhibits the highest torque coefficient across most advance ratios, except J=0.4. In the remaining cases, differences are observed within the J=0.4 to J=0.6 range, after which the values converge. All conditions show a descending trend, with fluctuations in the J=0.6 to J=0.8 range**.**

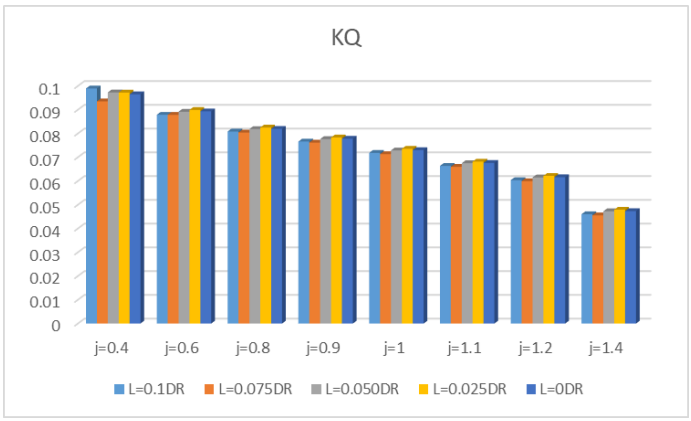

Figure 15: Comparative Bar Chart of Torque Coefficient for Five Investigated Conditions at Various Advance ratios.

6.4. Open Water Efficiency and Its Uncertainty Range

Figure 16 presents the calculated Open water efficiency for the five investigated conditions. An analysis of the results indicates that the L=0.1DR condition exhibits the highest Open water efficiency across most advance ratios, except 0.4.

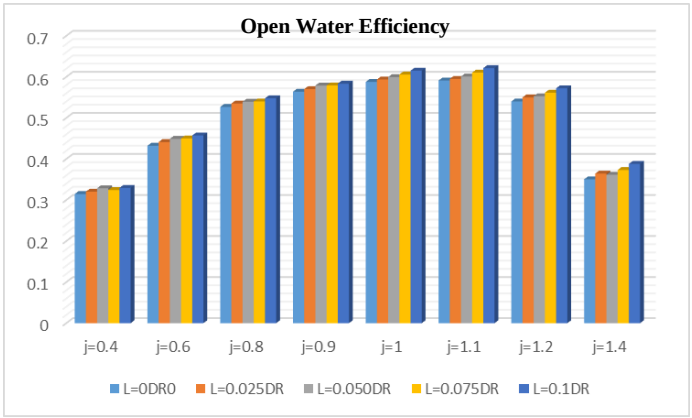

Figure 16: Comparative Bar Chart of Open water Efficiency for the Five Investigated Cases at Various Advance ratios.

The range of Open water efficiency uncertainty values for the five investigated cases at various advance ratios are presented in Figure 17. At an advance ratio of 0.4, the highest upper efficiency bound corresponds to the L=0.1DR condition. In contrast, the lowest lower bound is associated with the L=0.050DR condition, showing only a slight difference from the lower bound of the L=0.1DR condition. At advance, coefficients of

0.6, 1.1, and 1.4, the highest upper and lower bound of Open water efficiency correspond to the L=0.1DR condition. The maximum Open water efficiency for all five cases occurs at an advance ratio of 1.1, where the upper and lower bounds for the L=0.1DR condition exceed those of all other cases.

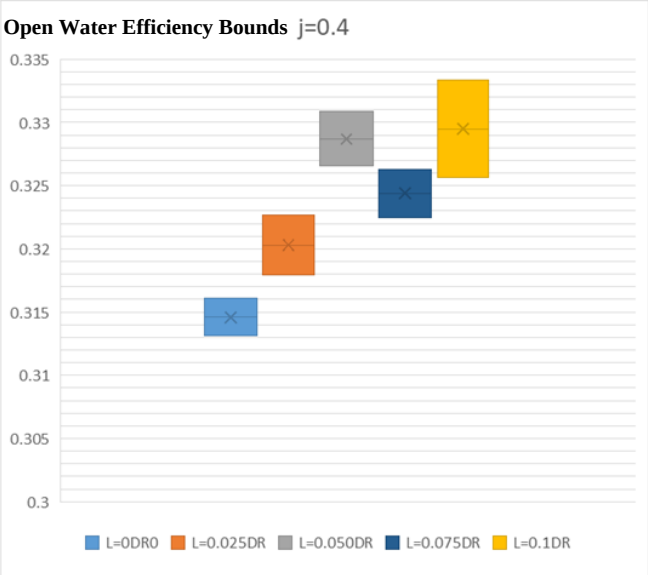

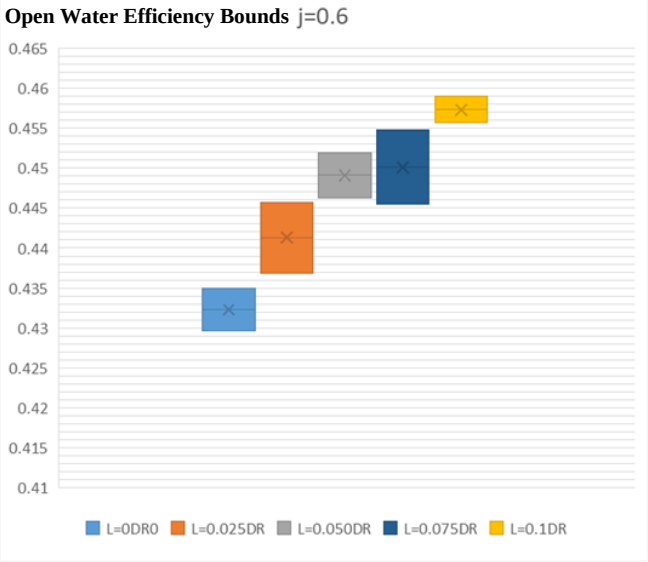

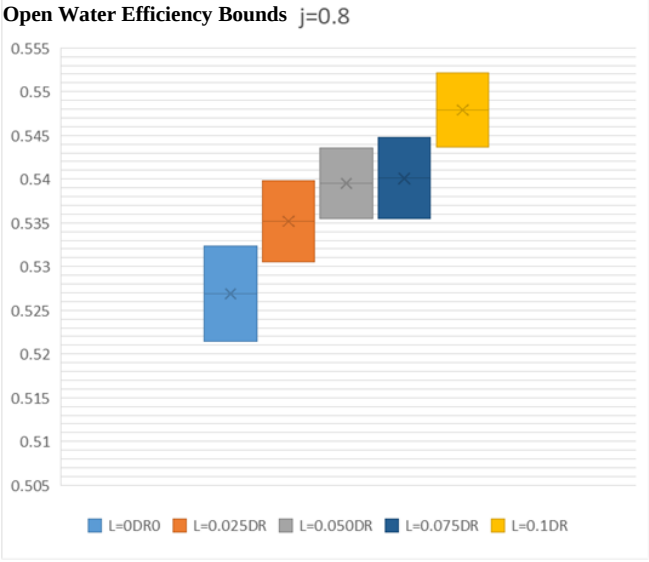

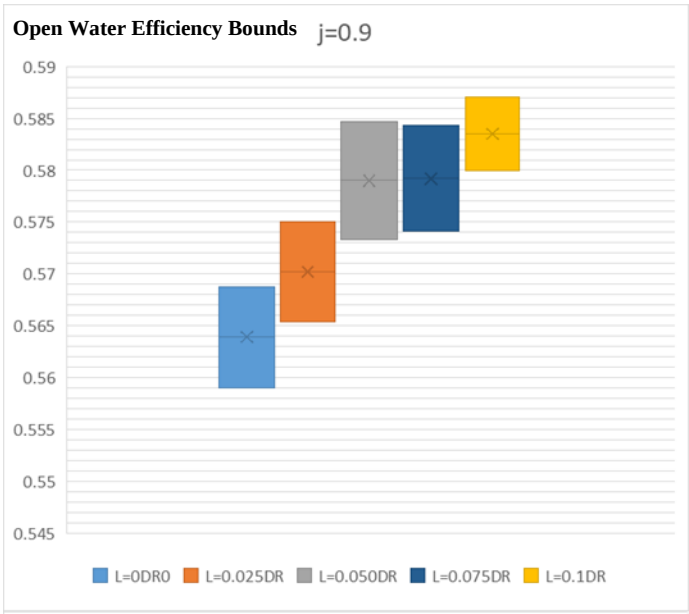

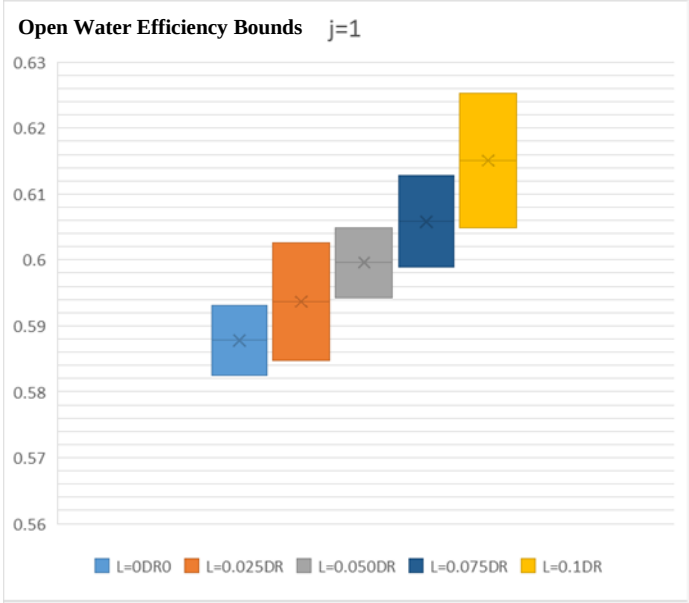

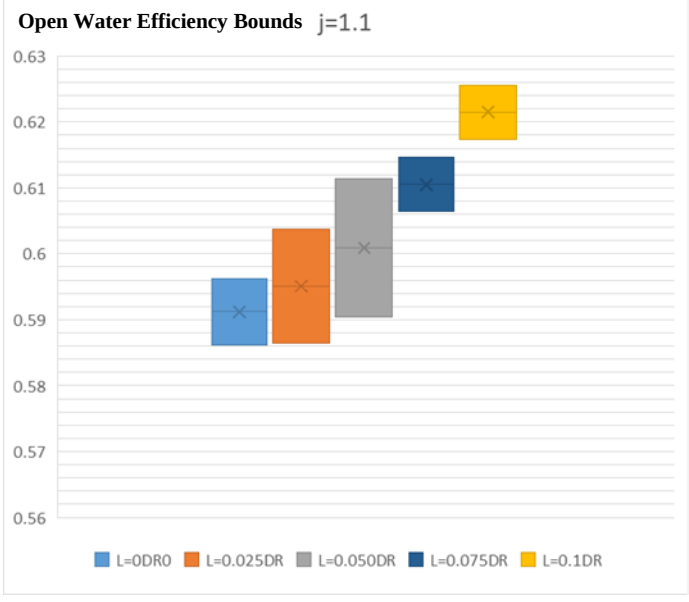

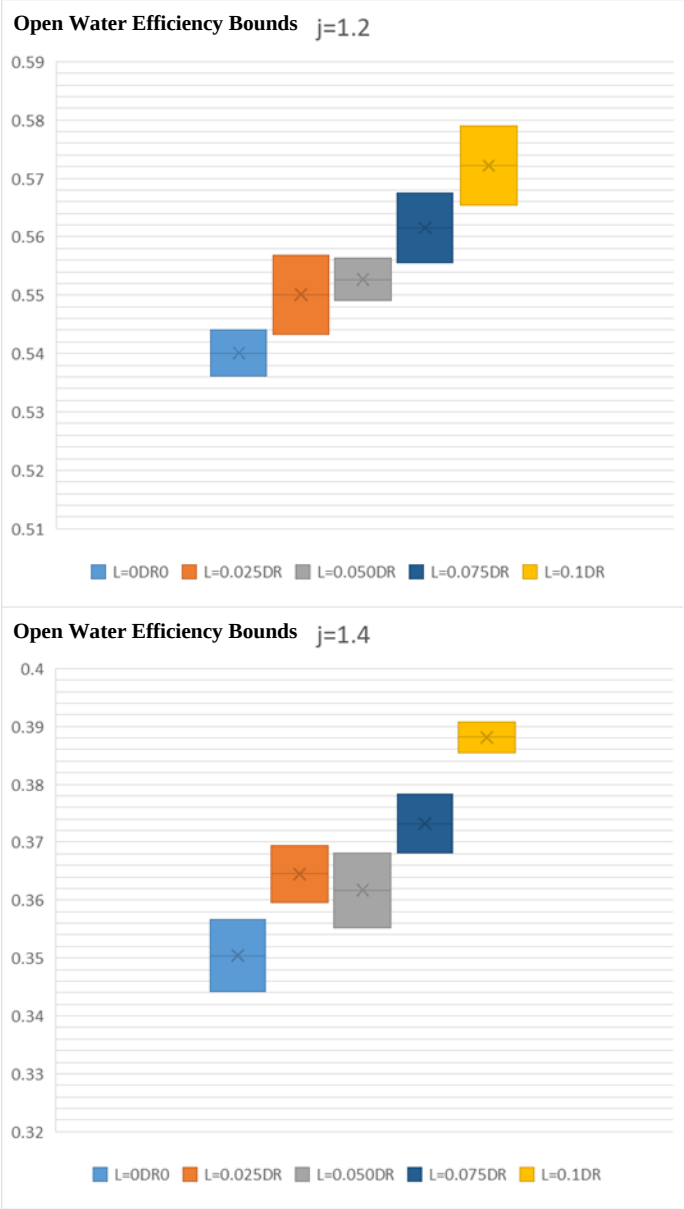

Figure 17: Comparative Bar Chart of Openwater Efficiency Ranges for Five Investigated Cases at Various Advance Ratios

7. Conclusion and Summary

Pre-swirl pumpjet systems are vital for underwater vehicles like submarines due to their high efficiency and low noise characteristics. This study utilizes both experimental methods and uncertainty analysis. It investigates the impact of duct inlet length on a pre-swirl pumpjet system's hydrodynamic performance, particularly the open water efficiency. Five configurations with varying duct inlet lengths (L=0DR, 0.025DR, 0.050DR, 0.075DR, and 0.1DR, where DR represents the rotor diameter) were tested in the cavitation tunnel at Imam Khomeini Naval University in Noshahr. Measured parameters included rotor thrust, stator duct assembly thrust, and rotor torque, each recorded at eight different advance ratios (J) and repeated four times.

The main findings of the research are as follows:

- Sensitivity and Uncertainty Analysis:

Sensitivity analysis revealed that rotor torque influences open water efficiency more than total thrust, underscoring the importance of accurate torque measurements. The uncertainty analysis showed that the relative efficiency uncertainty across all configurations was less than 1.794%, with the maximum value occurring at L=0.050DR and J=1.4. The L=0.1DR configuration exhibited the lowest uncertainty range, indicating the high precision of the experimental measurements for this condition.

- Thrust Coefficient: The total thrust coefficient decreases as J increases. The L=0.1DR configuration consistently had the highest value across the most advance ratios, suggesting that longer inlet lengths can generate greater thrust under specific conditions.
- Torque Coefficient: Similar to the thrust coefficient, the torque coefficient also shows a decreasing trend with increasing J.
- Open water Efficiency: Open water efficiency for all configurations reached its maximum at J=1.1 and decreased with further increases in J. The maximum efficiency values were:

L=0DR: 59.12%
L=0.025DR: 59.51%
L=0.050DR: 60.09%
L=0.075DR: 61.05%
L=0.1DR: 62.15%

The L=0.1DR configuration demonstrated the highest efficiency at 62.15%, representing a 5.15% improvement compared to L=0DR. This enhancement is attributed to increased thrust and reduced torque resulting from improved uniformity of the inlet flow to the stator and optimized angle of attack to the rotor blades.

- Open water Efficiency Uncertainty Range:

At advance ratios of 0.6, 1.1, and 1.4, the broadest range of open water efficiency corresponds to the L=0.1DR condition. For other advance ratios, the upper bound of open water efficiency also belongs to the L=0.1DR configuration. Therefore, based on the uncertainty analysis, the L=0.1DR condition performs better in open water efficiency than the other conditions.

7.1. Overall Conclusion:

7.1.1. Key Findings Summary:

This study demonstrates that increasing the duct inlet length significantly improves the open water efficiency of pre-swirl pumpjet systems, with the L=0.1DR configuration achieving the highest efficiency (62.15%) at J=1.1. This improvement is due to better uniformity of the inlet flow and optimized rotor blade angle of attack. The uncertainty analysis, with a

maximum relative uncertainty below 1.794%, confirmed the high accuracy of the results.

7.1.2. Scientific and Practical Implications:

These findings have important implications for the design of marine propulsion systems. Optimizing the duct inlet length can enhance hydrodynamic efficiency, crucial for underwater vehicles such as submarines and autonomous underwater vehicles (AUVs). These advancements can reduce energy consumption and contribute to global sustainability goals.

7.1.3. Future Research Directions

The experiments were conducted in a controlled cavitation tunnel environment, which may not fully replicate real-world effects such as wall effects and propeller wake. Future research should investigate these parameters under operational conditions and study noise generation and cavitation phenomena.

7.1.4 Final Summary

By providing a comprehensive analysis of the impact of duct inlet length, this study advances the understanding of pre-swirl pumpjet hydrodynamics and offers practical guidelines for designing more efficient propulsion systems. These findings contribute significantly to the progress of marine technology.

7.1.5. Acknowledgements

The authors express their sincere gratitude to the esteemed authorities of Imam Khomeini Naval University (RA) in Noshahr for their full cooperation in conducting the experimental tests.

8. Data Availability Statement

Authors should specify whether the data are shareable, where they can be accessed, or, if there are any restrictions, the reasons for those limitations.

9. References

[1] A comparison of pump jets and propellers for non-nuclear submarine propulsion Aidan Morrison January 2018

[2] Renilson MR (2018) Submarine hydrodynamics, 2nd edn. Springer, Cham.
https://doi.org/10.1007/978-3-319-79057-2

[3] A.Dean, D.Voss, Design and Analysis of Experiments, Springer Verlag: New York,1999.

[4] Insttrumentation Measurement And Analysis, 4Th Edn, by B.C. Nakra And K.K. Chaudhry.2016

[5]H.W.Coleman, W.G.Steele, Experimentation and Uncertainty Analysis for Engineers", John Wiley and Sons, Inc., New York.1999

[٦] Analysis of heat transfer and fuel regression rate of solid fuel in hybrid thrusters [M.Sc.Thesis], Researcher Mohammad Hossein Qaedsharaf, Islamic Azad University, Science & Research Branch, 2011

[7] Motallebi-Nejad, M., Bakhtiari, M., Ghassemi, H. et al. Numerical analysis of ducted propeller and pumpjet propulsion system using periodic computational domain. J Mar Sci Technol 22, 559–573 (2017).
https://doi.org/10.1007/s00773-017-0438-x

[٨] Ghaedsharf, Mohammad Hossein, Ehsan, Mahdavi, Hadi and Mehrabi Gohari. (2019). Comparison of performance and sensitivity of effective parameters in two propellants hydrogen peroxide and nitrous oxide using uncertainty analysis. Mechanical Engineering, University of Tabriz, 50(3), 233-237.
doi: https://10.22034/jmeut.2020.9802

[٩] Wang, C., Weng, K., Guo, C. et al. Analysis of influence of duct geometrical parameters on pump jet propulsor hydrodynamic performance. J Mar Sci Technol 25, 640–657 (2020).
https://doi.org/10.1007/s00773-019-00662-z

[١٠] Huang, Q., Li, H., Pan, G., & Dong, X. (2021). Effects of duct parameter on pump-jet propulsor unsteady hydrodynamic performance. Ocean Engineering, 221, 108509.
https://doi.org/10.1016/j.oceaneng.2020.108509

[١١] Chen, X., Cheng, L., Wang, C., & Luo, C. (2021). Influence of inlet duct length on the hydraulic performance of the waterjet propulsion device. *Shock and Vibration*, *2021*(1), 6676601.
https://doi.org/10.1155/2021/6676601

[١٢] Zhou, Y., Pavesi, G., Yuan, J., & Fu, Y. (2022). A Review on Hydrodynamic Performance and Design of Pump-Jet: Advances, Challenges and Prospects. Journal of Marine Science and Engineering, 10(10), 1514.
https://doi.org/10.3390/jmse10101514

[١٣] Zhou, Y., Pavesi, G., Yuan, J., Fu, Y., & Gao, Q. (2023). Effects of duct profile parameters on flow characteristics of pump-jet: A numerical analysis on accelerating and decelerating ducts distinguished by cambers and angles of attack. Ocean Engineering, 281, 114733.
https://doi.org/10.1016/j.oceaneng.2023.114733

[١٤] Ji, X. Q., Zhang, X. S., Yang, C. J., & Dong, X. Q. (2024). Experimental and numerical investigation of the impacts of rotor tip-rake on excitation forces of pump-jet propulsors. Journal of Hydrodynamics, 1-16.
https://doi.org/10.1007/s42241-024-0011-0

[١٥] Zou, D., Xue, L., Lin, Q., Xu, J., Dong, X., Ta, N., & Rao, Z. (2024). Influence of propulsion shafting longitudinal vibration on the excitation force and vortex dynamics characteristics of pump-jet propulsor. Ocean Engineering, 295, 116962.
https://doi.org/10.1016/j.oceaneng.2024.116962

[١٦] Weng, K., Sun, C., Han, K., Wang, C., Sun, S., Li, P., & Hu, J. (2024). Experimental/numerical investigation on the hydrodynamic and noise

characteristics of pump-jet propulsion. Ocean Engineering, 307, 117995.
https://doi.org/10.1016/j.oceaneng.2024.117995
[١7] Zhou, Y., Pavesi, G., Yuan, J., Fu, Y., & Gao, Q. (202٤). Effects of duct profile parameters on flow characteristics of pump-jet: A numerical analysis on accelerating and decelerating ducts distinguished by cambers and angles of attack. *Ocean Engineering, 281*, 114733.
https://doi.org/10.1016/j.oceaneng.2023.114733
[١٨] Qaedsharaf, M. H., Yari, E., & Manshadi, M. D. (2025). Cavitation on the pump jet pre swirl type due to changes in the stator chord length. Physics of Fluids, 37(3).
https://doi.org/10.1063/5.0248017
[١٩] Carlton, J. S., Marine propellers and propulsion, third ed., Amsterdam, Netherland, Elsevier (2012)
[٢٠] Bertram, V., Practical ship hydrodynamics Oxford, U.K, Butterworth Heinemann (2012)